

Exploring the three flavor effects with future superbeams using liquid argon detectors

Sanjib Kumar Agarwalla,^a Suprabh Prakash,^b S. Uma Sankar^b

^a*Institute of Physics, Sachivalaya Marg, Sainik School Post, Bhubaneswar 751005, India*

^b*Department of Physics, Indian Institute of Technology Bombay, Mumbai 400076, India*

E-mail: sanjib@iopb.res.in, suprabh@phy.iitb.ac.in, uma@phy.iitb.ac.in

ABSTRACT: Recent measurement of a moderately large value of θ_{13} signifies an important breakthrough in establishing the standard three flavor oscillation picture of neutrinos. It has provided an opportunity to explore the sub-dominant three flavor effects in present and future long-baseline experiments. In this paper, we perform a comparative study of the physics reach of two future superbeam facilities, LBNE and LBNO in their first phases of run, to resolve the issues of neutrino mass hierarchy, octant of θ_{23} , and leptonic CP violation. We also find that the sensitivity of these future facilities can be improved significantly by adding the projected data from T2K and NO ν A. Stand-alone LBNO setup with a 10 kt detector has a mass hierarchy discovery reach of more than 7σ , for the lowest allowed value of $\sin^2\theta_{23}(\text{true}) = 0.34$. This result is valid for any choice of true δ_{CP} and hierarchy. LBNE10, in combination with T2K and NO ν A, can achieve 3σ hierarchy discrimination for any choice of δ_{CP} , $\sin^2\theta_{23}$, and hierarchy. The same combination can provide a 3σ octant resolution for $\sin^2\theta_{23}(\text{true}) \leq 0.44$ or for $\sin^2\theta_{23}(\text{true}) \geq 0.58$ for all values of $\delta_{\text{CP}}(\text{true})$. LBNO can give similar results with 10 kt detector mass. In their first phases, both LBNE10 and LBNO with 20 kt detector can establish leptonic CP violation for around 50% values of true δ_{CP} at 2σ confidence level. In case of LBNE10, CP coverage at 3σ can be enhanced from 3% to 43% by combining T2K and NO ν A data, assuming $\sin^2\theta_{23}(\text{true}) = 0.5$. For LBNO setup, CP violation discovery at 3σ is possible for 46% values of true δ_{CP} if we add the data from T2K and NO ν A.

KEYWORDS: Neutrino Mass Hierarchy, Octant of θ_{23} , Leptonic CP violation, Long-baseline Experiments, Three Flavor Effects

ARXIV EPRINT: [1304.3251](https://arxiv.org/abs/1304.3251)

Contents

1	Introduction and Motivation	1
2	Platinum Channel: Test Bed for Three Flavor Effects	3
3	Experimental Specifications	4
3.1	Current Generation: T2K and NO ν A	4
3.2	Future Generation: LBNE and LBNO	5
4	Physics with Bi-events Plot	5
5	Our Findings	7
5.1	Discovery Reach for Neutrino Mass Hierarchy	7
5.2	Discovery Reach for θ_{23} Octant	9
5.3	Discovery Reach for Leptonic CP Violation	12
6	Concluding Remarks	14
A	Resolution of Octant as a function of true θ_{23} for IH(true)	15
B	CP Violation discovery as a function of true δ_{CP} for IH(true)	16

1 Introduction and Motivation

The discovery of neutrino oscillations over the past decade provides firm evidence for new physics. Recently, the unknown 1-3 lepton mixing angle has been measured quite precisely by the reactor experiments [1–4]. They have found a moderately large value, not too far from its previous upper bound. This represents a significant milestone towards addressing the remaining fundamental questions, in particular determining the neutrino mass hierarchy and searching for CP violation in the neutrino sector. Another recent and crucial development is the indication of non-maximal 2-3 mixing by the MINOS accelerator experiment [5, 6], leading to the problem of determining the correct octant of θ_{23} . It is possible to resolve all the above three issues by the observation of ν_e appearance via $\nu_\mu \rightarrow \nu_e$ oscillations. The determination of CP violation in particular requires the full interplay of three flavor effects in neutrino oscillations.

Oscillation data are insensitive to the lowest neutrino mass. However, it can be measured in tritium beta decay processes [7], neutrinoless double beta decay experiments [8], and from the contribution of neutrinos to the energy density of the universe [9]. Very recent data from the Planck experiment in combination with the WMAP polarization and baryon acoustic oscillation measurements have set an upper bound on the sum of all the neutrino

mass eigenvalues of $\sum m_i \leq 0.23$ eV at 95% C.L. [10]. But, oscillation experiments are capable of measuring the two independent mass-squared differences: $\Delta m_{21}^2 = m_2^2 - m_1^2$ and $\Delta m_{31}^2 = m_3^2 - m_1^2$. Δm_{21}^2 is required to be positive by the solar neutrino data but at present Δm_{31}^2 can be either positive or negative. Hence, two patterns of neutrino masses are possible: $m_3 > m_2 > m_1$, called normal hierarchy (NH) where Δm_{31}^2 is positive and $m_2 > m_1 > m_3$, called inverted hierarchy (IH) where Δm_{31}^2 is negative. Leptonic CP violation can be established if CP violating phase δ_{CP} in the mixing matrix, differs from both 0 and 180° . So far, there is no constraint on δ_{CP} . It can take any value in the range $[-180^\circ, 180^\circ]$. Regarding θ_{23} , all global fits [11–13] point to a deviation from maximal mixing (MM) *i.e.* $(0.5 - \sin^2 \theta_{23}) \neq 0$. This raises an additional question: “whether θ_{23} lies in the lower octant (LO: $\theta_{23} < 45^\circ$) or higher octant (HO: $\theta_{23} > 45^\circ$)?”.

Settling the issue of neutrino mass hierarchy is crucial to determine the structure of neutrino mass matrix. This structure will provide the fundamental input needed to develop the theory of neutrino masses and mixing [14]. Neutrino mass hierarchy is also a key parameter for neutrinoless double beta decay searches probing the Majorana nature of neutrinos [15]. Another fundamental issue that needs to be addressed in long-baseline experiments is to establish leptonic CP violation and measure δ_{CP} . This new CP violation in the lepton sector may be able to explain the observed matter anti-matter asymmetry in the universe via leptogenesis [16]. A number of innovative ideas, such as $\mu \leftrightarrow \tau$ symmetry [17], A_4 flavor symmetry [18], quark-lepton complementarity [19], and neutrino mixing anarchy [20, 21] have been invoked to explain the observed pattern of one small and two large mixing angles in the neutrino sector. Measurements of the precise values of θ_{13} and θ_{23} will reveal the pattern of deviations from these symmetries and will lead to a better understanding of neutrino masses and mixing. In particular, the resolution of θ_{23} octant will severely constrain the patterns of symmetry breaking. With the recent discovery of moderately large value of θ_{13} , these three fundamental measurements fall within our reach.

The combined data from the current ν_e appearance experiments, T2K [22, 23] and NO ν A [24–26], can provide a hint at 90% confidence level for neutrino mass ordering [27] and at 95% confidence level for octant of θ_{23} [28, 29]. They can determine these quantities at $> 99\%$ C.L. only for a very small range of favorable values of δ_{CP} . Discovery of leptonic CP violation is possible at 95% C.L. only for values of δ_{CP} close to $\pm 90^\circ$, *i.e.* where CP violation is maximum [27]. Hence, future facilities consisting of intense, high power wide-band beams and large smart detectors are mandatory to cover the entire parameter space at a high confidence level. In this paper, we explore the capabilities of future superbeam experiments with liquid argon detectors, LBNE [30–34] and LBNO [35–39] towards resolving these unknowns. We first present the stand-alone performances of these setups in their first phases. Then we examine how the addition of projected data from T2K and NO ν A, can improve the sensitivity of these future facilities. We also study in detail how these sensitivities change as the true value of $\sin^2 \theta_{23}$ varies in its allowed 3σ range of 0.34 to 0.67.

We start with a brief discussion of $\nu_\mu \rightarrow \nu_e$ oscillation channel in section 2. In section 3, we describe the important features of the experimental setups under consideration. Next, we introduce the concept of bi-events plots (ν_e vs. $\bar{\nu}_e$ appearance events) to explain the

underlying physics in section 4. In section 5, we present our results. Finally, we summarize and draw our conclusions in section 6.

2 Platinum Channel: Test Bed for Three Flavor Effects

A study of $\nu_\mu \rightarrow \nu_e$ and $\bar{\nu}_\mu \rightarrow \bar{\nu}_e$ oscillations at long-baseline superbeam experiments is the simplest way to probe three flavor effects, including sub-leading ones. Such a study is capable of achieving all the three objectives mentioned in section 1. An approximate analytic expression for the oscillation probability, $P_{\mu e}$, in matter [40–42], is given by

$$\begin{aligned}
P_{\mu e} \simeq & \underbrace{\sin^2 \theta_{23} \sin^2 2\theta_{13} \frac{\sin^2[(1 - \hat{A})\Delta]}{(1 - \hat{A})^2}}_{C_0} + \underbrace{\alpha^2 \cos^2 \theta_{23} \sin^2 2\theta_{12} \frac{\sin^2(\hat{A}\Delta)}{\hat{A}^2}}_{C_1} \\
& - \underbrace{\alpha \sin 2\theta_{13} \cos \theta_{13} \sin 2\theta_{12} \sin 2\theta_{23} \sin(\Delta) \frac{\sin(\hat{A}\Delta)}{\hat{A}} \frac{\sin[(1 - \hat{A})\Delta]}{(1 - \hat{A})}}_{C_-} \sin \delta_{\text{CP}} \\
& + \underbrace{\alpha \sin 2\theta_{13} \cos \theta_{13} \sin 2\theta_{12} \sin 2\theta_{23} \cos(\Delta) \frac{\sin(\hat{A}\Delta)}{\hat{A}} \frac{\sin[(1 - \hat{A})\Delta]}{(1 - \hat{A})}}_{C_+} \cos \delta_{\text{CP}}, \quad (2.1)
\end{aligned}$$

where

$$\Delta \equiv \frac{\Delta m_{31}^2 L}{4E}, \quad \hat{A} \equiv \frac{A}{\Delta m_{31}^2}, \quad A = \pm 2\sqrt{2}G_F N_e E. \quad (2.2)$$

Equation 2.1 has been derived under the constant matter density approximation, keeping terms only up to second order in the small quantities θ_{13} and $\alpha \equiv \Delta m_{21}^2 / \Delta m_{31}^2$ [43–45]. Here, A is the matter potential, expressed in terms of the electron density, N_e , and the (anti-)neutrino energy E . It is positive for neutrinos and negative for anti-neutrinos. For anti-neutrinos, the term proportional to $\sin \delta_{\text{CP}}$ has the opposite sign. So far, it was possible to analyze the data from each oscillation experiment using an appropriate, effective two flavor oscillation approach because of the smallness of the mixing angle $\sin 2\theta_{13} \simeq 0.3$ and the ratio $\alpha \simeq 0.03$. This method has been quite successful in measuring the solar and atmospheric neutrino parameters. The next step must involve probing the full three flavor effects, including the sub-leading ones proportional to α . This task will be undertaken, for the first time, by the current generation experiments T2K and NO ν A.

In this paper, we consider two future long-baseline superbeam experiments with large matter effect. The matter effect increases $P(\nu_\mu \rightarrow \nu_e)$ oscillation probability for NH and decreases it for IH. For anti-neutrinos the situation is reversed. It can be seen from equation 2.1 that the dominant term (C_0) is driven by matter modified Δm_{31}^2 and is proportional to $\sin^2 \theta_{23} \sin^2 2\theta_{13}$ but the sub-dominant δ_{CP} dependent terms (C_- & C_+) are suppressed by α . Since the hierarchy and δ_{CP} are both unknown, the interplay of the terms C_0 , C_- , and C_+ in equation 2.1 gives rise to hierarchy- δ_{CP} degeneracy [46]. If the matter effects

are large enough, this degeneracy can be broken completely. This is *not* the case for T2K and NO ν A, because of which their sensitivity to hierarchy is modest for about half the δ_{CP} range. There is a similar octant- δ_{CP} degeneracy also, which limits our ability to determine the correct octant of θ_{23} . This problem can be solved by having substantial data in both ν and $\bar{\nu}$ channels [28]. Both the future facilities, LBNE (baseline of 1300 km) and LBNO (baseline of 2290 km) will operate at multi-GeV energies with very long-baselines. This will lead to a large enough matter effect which breaks the hierarchy- δ_{CP} degeneracy completely. They are also scheduled to have equal ν and $\bar{\nu}$ runs, and can resolve the octant- δ_{CP} degeneracy effectively. These experiments are planning to use liquid argon time projection chambers (LArTPCs) which have excellent kinematic reconstruction capability for all the observed particles. This feature helps in rejecting almost all of the large neutral current background.

3 Experimental Specifications

In this section, we briefly describe the key experimental features of the current (off-axis) and future (on-axis) generation long-baseline superbeamed experiments that we use in our simulation.

3.1 Current Generation: T2K and NO ν A

In Japan, the Tokai-to-Kamioka (T2K) experiment [22, 23] started taking data in 2010. The NO ν A experiment [24–26] in the United States is now under construction and will start taking data near the end of this year. The main goal of these experiments is to detect the electron neutrino appearance events in a ν_{μ} beam using the classic off-axis beam technique [47] that delivers a beam with a narrow peak in the energy spectrum. The position of this peak is tuned to be close to the expected oscillation maximum. In our study, we have explored the improvement in the physics capabilities of LBNE and LBNO in their first phases, due to the addition of the projected data from T2K and NO ν A experiments.

In the T2K experiment, a 2.5° off-axis ν_{μ} beam from J-PARC is observed in the Super-Kamiokande detector (fiducial volume 22.5 kt) at Kamioka, at a distance of 295 km [22]. The neutrino flux peaks sharply at the first oscillation maximum of 0.6 GeV. For mass hierarchy and CP violation studies, we consider 5 years of neutrino run with a beam power of 0.75 MW as officially announced. Recently, it has been shown in reference [28] that equal runs in neutrino and anti-neutrino modes in T2K experiments are vital to settle the octant ambiguity of θ_{23} for all values of δ_{CP} . Therefore, we assume equal neutrino and anti-neutrino runs of 2.5 years each for the T2K while exploring the octant sensitivity. The signal efficiency in T2K is around 87%. In our simulation, the background information and other details for T2K experiment are taken from [48, 49].

In the NO ν A experiment, the NuMI beam will be sent towards a 14 kt totally active scintillator detector (TASD) placed at a distance of 810 km from Fermilab, at a location which is 0.8° off-axis from the beam. Due to the off-axis location, the flux is sharply peaked around 2 GeV, again close to the first oscillation maximum in $P(\nu_{\mu} \rightarrow \nu_e)$ channel. The experiment is scheduled to have three years run in neutrino mode first and then later, three

years run in anti-neutrino mode. The NuMI beam power is 0.7 MW, which corresponds to 6×10^{20} protons on target (p.o.t.) per year. See, reference [26] for details. After the discovery of moderately large value of θ_{13} , NO ν A has reoptimized its event selection criteria. A few cuts have been relaxed to allow more events in both signal and background. Additional neutral current backgrounds are reconstructed at lower energies and can be rejected by a kinematical cut. In our simulation, we use all these new features, the details of which are given in [27, 50].

3.2 Future Generation: LBNE and LBNO

The Long-Baseline Neutrino Experiment (LBNE) [33, 34] is one of the major components of Fermilab’s intensity frontier program. In its first phase (LBNE10), it will have a new, high intensity, on-axis neutrino beam directed towards a 10 kt LArTPC located at Homestake with a baseline of 1300 km. This facility is designed for initial operation at a proton beam power of 708 kW, with proton energy of 120 GeV that will deliver 6×10^{20} p.o.t. in 230 days per calendar year. In our simulation, we have used the latest fluxes being considered by the collaboration, which have been estimated assuming the smaller decay pipe and the lower horn current compared to the previous studies [51]. We have assumed five years each of ν and $\bar{\nu}$ runs. The detector characteristics have been taken from Table 1 of [52]. To have the LArTPC cross-sections, we have scaled the inclusive charged current (CC) cross sections of water by 1.06 (0.94) for the ν ($\bar{\nu}$) case [53, 54].

The Long-Baseline Neutrino Oscillation Experiment (LBNO) [39] plans to use an experimental set-up where neutrinos produced in a conventional wide-band beam facility at CERN would be observed in a proposed 20 kt (in its first phase) LArTPC housed at the Pyhäsalmi mine in Finland, at a distance of 2290 km. The fluxes have been computed [55] assuming an exposure of 1.5×10^{20} p.o.t. in 200 days per calendar year from the SPS accelerator at 400 GeV with a beam power of 750 kW. For LBNO also, we consider five years each of ν and $\bar{\nu}$ runs. We assume the same detector properties as that of LBNE10. In our calculations, we also consider a LBNO configuration reducing the detector mass to 10 kt which we denote as 0.5*LBNO. The exposure for this setup will be quite similar to LBNE10 which will enable us to perform a comparative study between these two setups at the same footing. The results presented in this paper are obtained using the GLoBES software [56, 57].

4 Physics with Bi-events Plot

In this section, we attempt to understand the physics capabilities of 0.5*LBNO and LBNE10 setups with the help of bi-events plot. This kind of plot is quite useful to get a qualitative estimate of the physics sensitivity before performing a full $\Delta\chi^2$ calculation. In figure 1, we have plotted ν_e vs. $\bar{\nu}_e$ appearance events, for 0.5*LBNO and LBNE10 for the four possible combinations of hierarchy and octant. Since δ_{CP} is unknown, events are generated for the full range $[-180^\circ, 180^\circ]$, leading to the ellipses. The event rates are calculated using the following oscillation parameters: $\Delta m_{21}^2 = 7.5 \times 10^{-5}$ eV², $\sin^2 \theta_{12} = 0.3$ [13], $\Delta m_{\text{eff}}^2 = \pm 2.4 \times 10^{-3}$ eV² [6], and $\sin^2 2\theta_{13} = 0.089$ [2]. Δm_{eff}^2 is the effective mass-squared

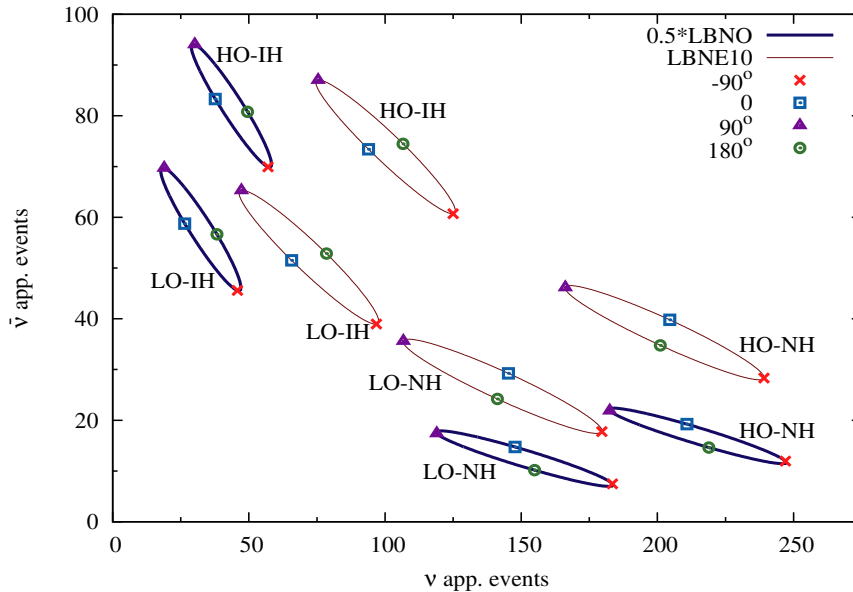


Figure 1: Bi-events (ν_e and $\bar{\nu}_e$ appearance) plot for the four possible octant-hierarchy combinations and all possible δ_{CP} values. The experiments considered are LBNE10 and 0.5*LBNO. Here $\sin^2 2\theta_{13} = 0.089$. For LO (HO), $\sin^2 \theta_{23} = 0.41(0.59)$.

difference measured using the ν_μ survival probability and is a linear combination of Δm_{31}^2 and Δm_{21}^2 . The value of Δm_{31}^2 is derived from Δm_{eff}^2 using the relation given in [58, 59]. This relation leads to different magnitudes of Δm_{31}^2 for NH and for IH. For $\sin^2 \theta_{23}$, we choose the two degenerate best-fit values of the global fit [13]: 0.41 in the lower octant (LO) and 0.59 in the higher octant (HO). Note that, here we have plotted the total number of events, whereas the actual analysis will be done based on the spectral information. Nevertheless, the contours in this figure contain very important information regarding the physics capabilities of the experiments. An experiment can determine both the hierarchy and the octant, if every point on a given ellipse is well separated from every point on each of the other three ellipses. The larger the separation, the better is the confidence level with which the above parameters can be determined.

One can see from figure 1 that for 0.5*LBNO, the two (LO/HO)-IH ellipses are well separated from the two (LO/HO)-NH ellipses, in number of ν_e events. Hence, 0.5*LBNO has excellent hierarchy determination capability with just ν data. However, ν data alone will not be sufficient to determine the octant in case of IH, because various points on (LO/HO)-IH ellipses have the same number of ν_e events. Likewise, only $\bar{\nu}$ data cannot determine the octant in case of NH. Therefore, balanced ν and $\bar{\nu}$ data are mandatory to make an effective distinction between (LO/HO)-IH ellipses and also between (LO/HO)-NH ellipses. Figure 1 also depicts that the asymmetries between the neutrino and anti-neutrino appearance events are largest for the combinations: (NH, $\delta_{\text{CP}} = -90^\circ$) and (IH, $\delta_{\text{CP}} = 90^\circ$).

For LBNE10, ν data alone can not determine hierarchy because various points on LO-NH and HO-IH ellipses have the same number of ν_e events (see figure 1). Thus, $\bar{\nu}$ data is

also needed. Even with $\bar{\nu}$ data, hierarchy determination can be difficult to achieve, if nature chooses LO and one of the two worst case combinations of hierarchy and δ_{CP} which are (NH, 90°) or (IH, -90°). In such a situation, the ν_e and $\bar{\nu}_e$ events are rather close to each other and it will be very difficult for LBNE10 to reject the wrong combination. Regarding octant determination, the capability of LBNE10 is very similar to that of 0.5*LBNO because the separations between the ellipses, belonging to LO and HO are very similar for these two experiments.

5 Our Findings

Measurement of mass hierarchy and octant should be considered as a prerequisite for the discovery of leptonic CP violation. Now, it would be quite interesting to study whether the expected appearance data from the first phases of LBNE and LBNO experiments can resolve the issues of neutrino mass hierarchy and octant of θ_{23} at 3σ to 5σ confidence level before they start probing the parameter space for leptonic CP violation. In this section, we address these issues in detail. We present the results for LBNE10 (10 kt), 0.5*LBNO (10 kt), and LBNO (20 kt) setups. We also study the improvement in their physics reach when the projected data from current generation experiments T2K and NO ν A, is added. The impact of T2K and NO ν A measurements on the performance of LBNE setup to determine the mass hierarchy and discover leptonic CP violation has been discussed recently in [60].

5.1 Discovery Reach for Neutrino Mass Hierarchy

We first focus on the discovery potential of future facilities to exclude the wrong hierarchy. It can be seen from equation 2.2 that the first term (C_0) dominates for large θ_{13} and it is the leading term in platinum channel. This term contains the largest Earth matter effect which can therefore be used to unravel the sign of Δm_{31}^2 . This term is also proportional to $\sin^2 \theta_{23}$ and therefore is quite sensitive to the choice of θ_{23} value. If we vary $\sin^2 \theta_{23}$ in its 3σ allowed range of 0.34 to 0.67, then for LBNE10, the signal event rates in ν_e appearance channel will increase from 122 to 231 (assuming NH and $\delta_{\text{CP}} = 0^\circ$), an almost $\sim 90\%$ enhancement in the statistics. For LBNO setup with 20 kt detector size, these numbers will change from 247 to 478 showing an almost $\sim 94\%$ increase in the event numbers. $\Delta\chi^2$ is calculated for a given true combination of θ_{23} -hierarchy, assuming the opposite hierarchy to be the test hierarchy. In the fit, we marginalize over test $\sin^2 \theta_{23}$ in its 3σ range. Δm_{eff}^2 and $\sin^2 2\theta_{13}$ are marginalized in their 2σ ranges. We consider 5% uncertainty in the matter density, ρ . Priors were added for ρ ($\sigma = 5\%$), Δm_{eff}^2 ($\sigma = 4\%$), and $\sin^2 2\theta_{13}$ ($\sigma = 5\%$, as expected by the end of Daya Bay's run [61]). $\Delta\chi^2$ is also marginalized over the uncorrelated systematic uncertainties (5% on signal and 5% on background) in the set-ups, so as to obtain a $\Delta\chi_{\text{min}}^2$ for every $\delta_{\text{CP}}(\text{true})$.

First, we consider two true values of $\sin^2 \theta_{23}$: 0.41 (best-fit value in LO) and 0.5 (MM) giving us four true combinations of θ_{23} -hierarchy: LO-NH, LO-IH, MM-NH and MM-IH. The hierarchy reach would suffer the most if $\sin^2 \theta_{23}(\text{true})$ belongs to LO, hence we show the results for the best-fit value in LO. Here, we would like to mention that if we take $\sin^2 \theta_{23}(\text{true})$ to be the best-fit value in HO, then the discovery reaches of these

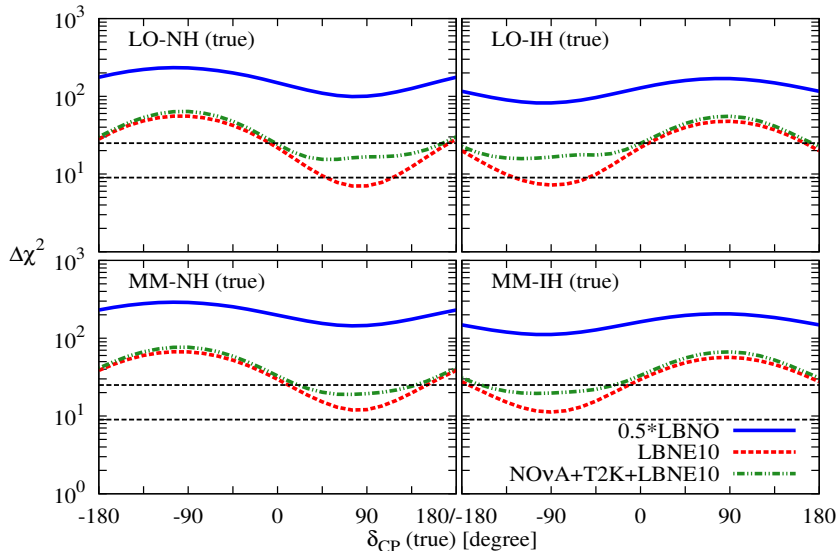


Figure 2: Discovery reach for mass hierarchy as a function of true δ_{CP} for 0.5*LBNO, LBNE10, and LBNE10 combining the projected data from T2K and NO ν A (see section 3). Results are shown for four possible true θ_{23} -hierarchy combinations. For LO (MM), $\sin^2 \theta_{23}(\text{true}) = 0.41$ (0.5). Here $\sin^2 2\theta_{13}(\text{true}) = 0.089$.

experiments will be better than that for the case of MM. We elaborate on this point at the end of this section. Figure 2 depicts the discovery reach for hierarchy as a function of $\delta_{\text{CP}}(\text{true})$. We see that even 0.5*LBNO has $\gtrsim 10\sigma^1$ hierarchy discovery potential for all values of $\delta_{\text{CP}}(\text{true})$ and for all four true θ_{23} -hierarchy combinations. The potential of LBNO, of course, is even better. The LBNO baseline is close to bimagic which gives it a particular advantage [63, 64]. For LBNE10, a 5σ discovery of hierarchy is possible for only $\sim 50\%$ of the $\delta_{\text{CP}}(\text{true})$, irrespective of these four true θ_{23} -hierarchy combinations. For the unfavorable hierarchy- δ_{CP} combinations [65], *i.e.* NH with δ_{CP} in the upper half plane or IH with δ_{CP} in the lower half plane, the performance of LBNE10 suffers. In particular, for LO and the worst case combinations [(NH, 90°) and (IH, -90°)], LBNE10 will not be able to provide even a 3σ hierarchy discrimination. This suggests that additional data is needed for LBNE10 to have such a capability. In such a scenario, the projected data from T2K and NO ν A can come to the rescue. Adding data from T2K (5 years of neutrino run) and NO ν A (3 years of ν run and 3 years of $\bar{\nu}$ run) helps LBNE10 setup to achieve more than 3σ discovery reach for mass hierarchy irrespective of the true choices of hierarchy and δ_{CP} (see upper panels of figure 2), even if θ_{23} is in the lower octant.

Now, we ask the question, by how much does the sensitivity deteriorate if $\sin^2 \theta_{23}(\text{true})$ turns out to be 0.34 in nature, which is its minimum value allowed in the 3σ range? We have

¹To estimate this, we use the relation $n\sigma = \sqrt{\Delta\chi_{\text{min}}^2}$. However, in order to calculate the sensitivity to the mass hierarchy, a new method has been described in [62] considering the fact that a discrete parameter does not follow a Gaussian distribution.

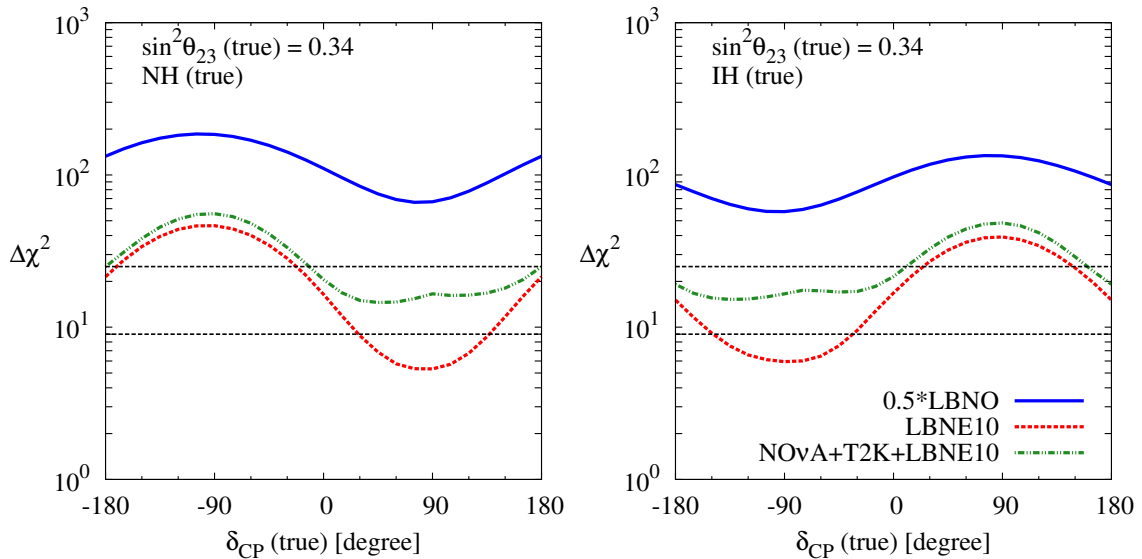


Figure 3: Left panel (right panel) shows the $\Delta\chi^2$ for the mass hierarchy discovery as a function of true value of δ_{CP} assuming NH (IH) as true hierarchy. Results are shown for 0.5*LBNO, LBNE10, and LBNE10+T2K+NO ν A. Here we consider $\sin^2\theta_{23}(\text{true}) = 0.34$ (the lowest value in its allowed 3σ range).

checked that even in this case, LBNO setup with 20 kt detector mass can give $\Delta\chi_{\text{min}}^2 \gtrsim 100$ irrespective of the true choices of hierarchy, and δ_{CP} . From figure 3, it can be seen that 0.5*LBNO can resolve the issue of mass hierarchy at more than 7σ confidence level for $\sin^2\theta_{23}(\text{true}) = 0.34$ independent of the choices of true hierarchy and δ_{CP} . The most important message that is conveyed by figure 3 is that with the help of projected T2K and NO ν A data, LBNE10 can still achieve 3σ mass hierarchy discovery for any combinations of true hierarchy- δ_{CP} - $\sin^2\theta_{23}$. It clearly demonstrates the synergy between the current (off-axis) and future (on-axis) superbeam experiments and also proves that adding data from three different baselines (295 km, 810 km, and 1300 km) with completely different energy spectra is quite useful to kill the clone solutions for the unfavorable choices of the oscillation parameters.

The mass hierarchy discovery potential for all the three set-ups under consideration is remarkable if θ_{23} happens to lie in HO. For $\sin^2\theta_{23}(\text{true}) = 0.59$ (the best-fit value in HO), even 0.5*LBNO can have $\Delta\chi_{\text{min}}^2 \gtrsim 130$ irrespective of the true choices of hierarchy and δ_{CP} . With this choice of $\sin^2\theta_{23}(\text{true})$, a 5σ discovery is not possible with LBNE10 for $\sim 30\%$ values of true δ_{CP} in the upper half plane for NH true and for $\sim 70\%$ values of true δ_{CP} in the lower half plane for IH true. We have checked that if we add the data from T2K and NO ν A, LBNE10 can again provide 5σ discovery for mass hierarchy irrespective of the choices of true hierarchy and δ_{CP} with $\sin^2\theta_{23}(\text{true}) = 0.59$. Next we turn our attention to the octant discovery potential of these setups.

5.2 Discovery Reach for θ_{23} Octant

Here we discuss the discovery reach of future facilities for excluding the wrong octant. We consider the best-fit true values of $\sin^2\theta_{23} = 0.41$ (in LO) and 0.59 (in HO) resulting into

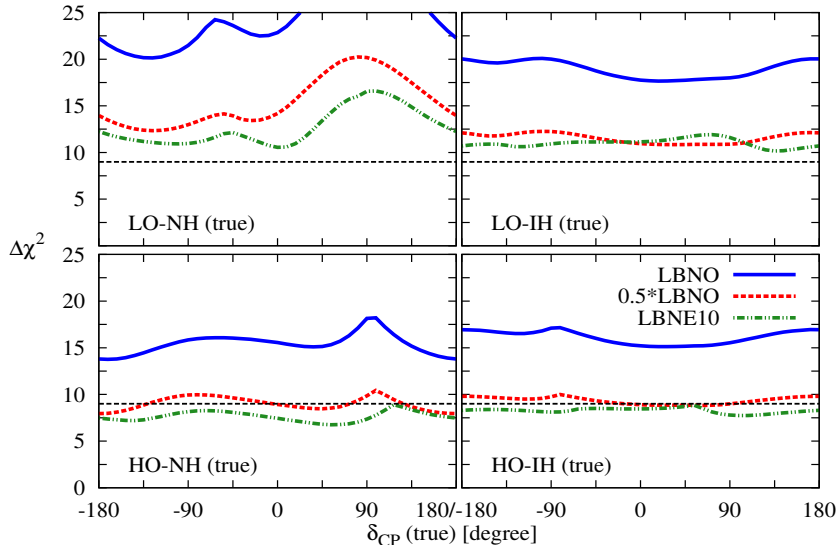


Figure 4: Octant resolving capability as a function of true δ_{CP} for LBNO, 0.5*LBNO, and LBNE10. Results are shown for the four possible true octant-hierarchy combinations. For LO (HO), $\sin^2 \theta_{23}(\text{true}) = 0.41$ (0.59). Here $\sin^2 2\theta_{13}(\text{true}) = 0.089$.

the following four true combinations of octant and hierarchy: LO-NH, LO-IH, HO-NH, and HO-IH. $\Delta\chi^2$ is calculated for each of these four combinations, assuming test $\sin^2 \theta_{23}$ values from the other octant. For LO (HO) true, we consider the test $\sin^2 \theta_{23}$ range from 0.5 to 0.67 (0.34 to 0.5). Rest of the marginalization procedure (over other oscillation parameters and systematic uncertainties) is the same as that in the case of hierarchy exclusion except with another difference: the final $\Delta\chi^2$ is marginalized over both the hierarchies in the fit to obtain $\Delta\chi_{\text{min}}^2$.

Figure 4 shows the discovery reach for octant as a function of $\delta_{\text{CP}}(\text{true})$. It can be seen that for (LO/HO)-IH true, the sensitivities of LBNE10 and 0.5*LBNO are quite similar whereas they are somewhat better for 0.5*LBNO if (LO/HO)-NH are the true combinations. For LO-(NH/IH), both LBNE10 and 0.5*LBNO have more than 3σ discovery of octant while for HO-(NH/IH), the $\Delta\chi_{\text{min}}^2$ varies from ~ 7 to 11 depending on the true value of δ_{CP} . However, with full LBNO, we have more than 3.5σ discovery of octant for all true octant-hierarchy- δ_{CP} combinations. A 5σ discovery of octant is possible only for LO-NH true for $\delta_{\text{CP}}(\text{true}) \in (\sim 20^\circ \text{ to } 150^\circ)$.

In figure 5, we present the improvement in the octant discovery reach for 0.5*LBNO and LBNE10 with the addition of the projected data from T2K (2.5 years of ν run and 2.5 years of $\bar{\nu}$ run) and NO ν A (3 years of ν run and 3 years of $\bar{\nu}$ run). Adding data from current generation experiments helps both 0.5*LBNO and LBNE10 to achieve more than 3σ discovery for all true octant-hierarchy- δ_{CP} combinations. For LO-(NH/IH) true, these setups can provide close to 3.8σ discovery for octant irrespective of the choice of true δ_{CP} .

In the discussion so far, we consider only the best-fit true values of $\sin^2 \theta_{23}$ in both

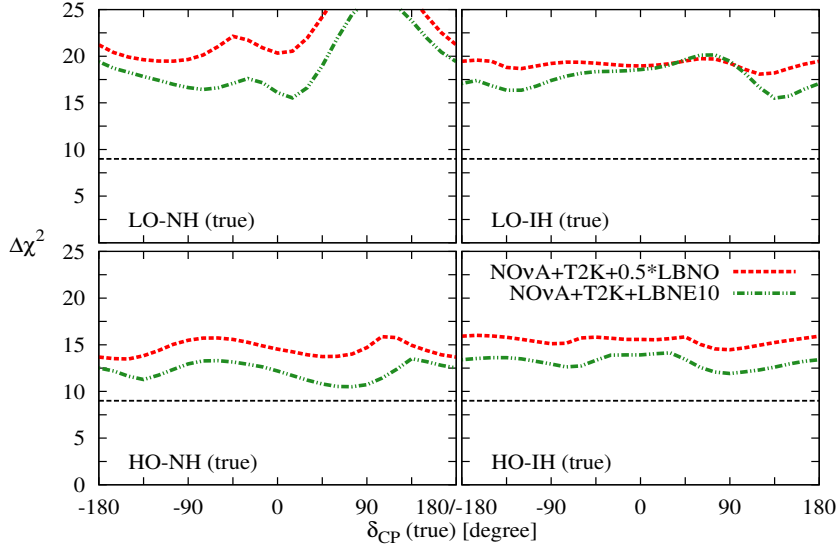


Figure 5: $\Delta\chi^2_{\min}$ for octant discovery potential as a function of true δ_{CP} for 0.5*LBNO and LBNE10 adding the projected data from T2K and NO ν A. Results are shown for the four possible true octant-hierarchy combinations. For LO (HO), $\sin^2\theta_{23}(\text{true}) = 0.41$ (0.59). Here $\sin^2 2\theta_{13}(\text{true}) = 0.089$.

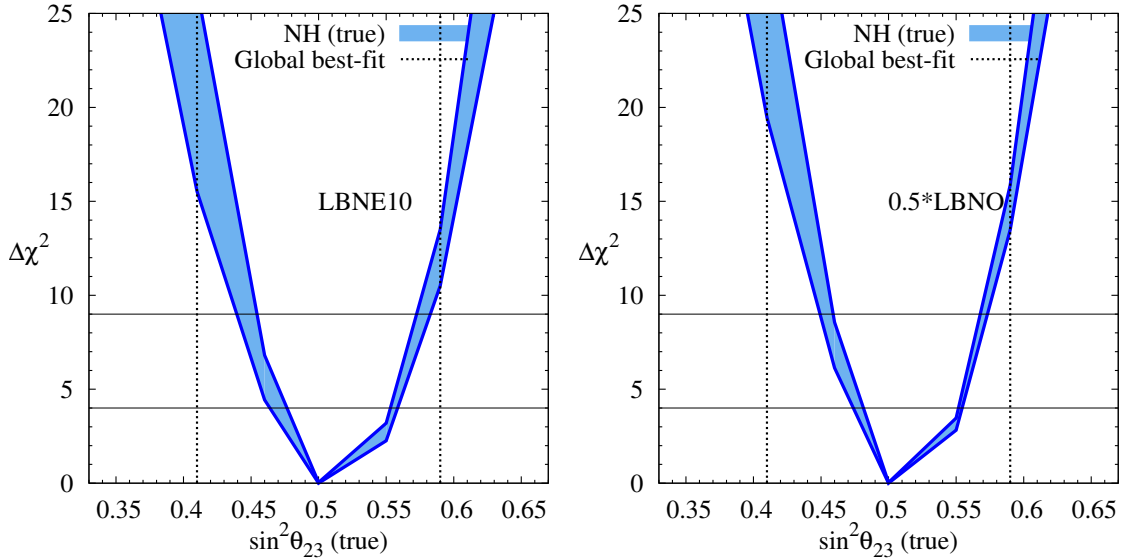


Figure 6: $\Delta\chi^2_{\min}$ for octant resolution as a function of true $\sin^2\theta_{23}$. Left panel (right panel) is for LBNE10 (0.5*LBNO). The variation due to $\delta_{\text{CP}}(\text{true})$ leads to the band in $\Delta\chi^2$ for a given $\sin^2\theta_{23}(\text{true})$. The vertical lines correspond to the global best-fit values. We consider NH as true hierarchy. In producing all these plots, the projected data from T2K and NO ν A have been added (see section 3 for details).

the octants. Now, we address the octant resolution capability for values of true $\sin^2\theta_{23}$ in the full 3σ allowed range of 0.34 to 0.67. In figure 6, we plot the $\Delta\chi^2_{\min}$ as a function of true $\sin^2\theta_{23}$ for LBNE10 (left panel) and 0.5*LBNO (right panel) assuming NH as true

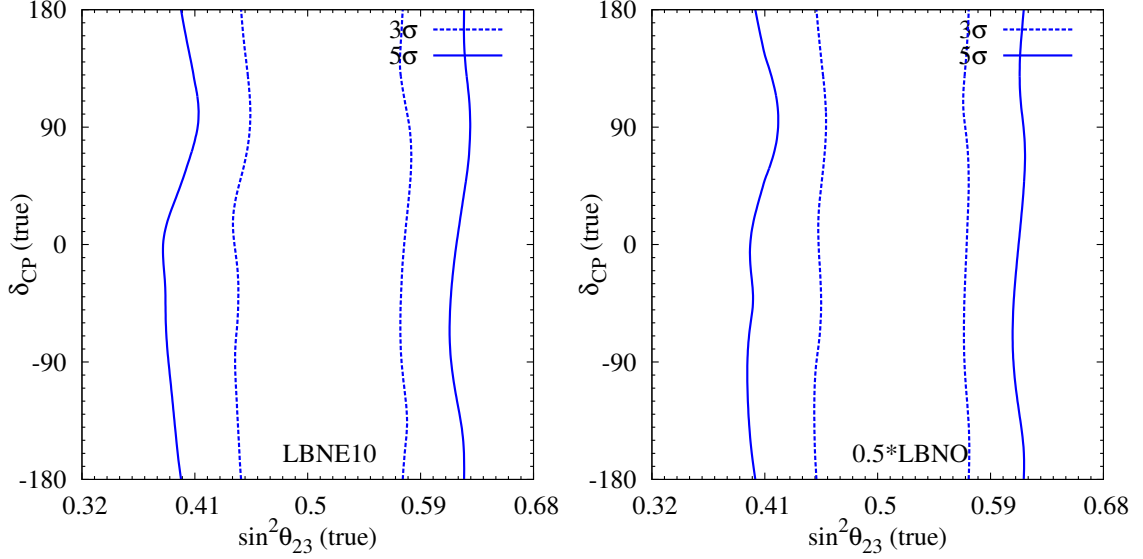


Figure 7: Octant resolving capability at 3σ and 5σ C.L. in the true $\sin^2\theta_{23}$ - true δ_{CP} plane for LBNE10 (left panel) and $0.5*\text{LBNO}$ (right panel). The vertical lines point towards the global best-fit values. Here, we assume NH as true hierarchy. In generating all these plots, the projected data from T2K and $\text{NO}\nu\text{A}$ have been added (see section 3 for details).

hierarchy. Variation of $\delta_{\text{CP}}(\text{true})$ in the range -180° to 180° leads to the band in $\Delta\chi^2$ values for a given true $\sin^2\theta_{23}$. The vertical lines point towards the global best-fit values. Here we have added the projected data from T2K and $\text{NO}\nu\text{A}$ to produce these results. For LBNE10, a 3σ octant resolution is possible for $\sin^2\theta_{23}(\text{true}) \leq 0.44$ and for $\sin^2\theta_{23}(\text{true}) \geq 0.58$ for all values of $\delta_{\text{CP}}(\text{true})$. For $0.5*\text{LBNO}$, this is possible for $\sin^2\theta_{23}(\text{true}) \leq 0.45$ and for $\sin^2\theta_{23}(\text{true}) \geq 0.57$. We present the results for IH as true choice in appendix A.

Figure 7 depicts the 3σ and 5σ octant resolution contours in true $\sin^2\theta_{23}$ - true δ_{CP} plane assuming NH as true hierarchy. The left (right) panel is for LBNE10 ($0.5*\text{LBNO}$) adding the expected data from T2K and $\text{NO}\nu\text{A}$. Octant resolution is only possible for points lying outside the contours. This figure again confirms that both LBNE10 and $0.5*\text{LBNO}$ in combination with T2K and $\text{NO}\nu\text{A}$ data can provide octant discovery for global best-fit points at 3σ confidence level. We show the similar figure for the true IH choice in appendix A.

5.3 Discovery Reach for Leptonic CP Violation

A ‘discovery’ of leptonic CP violation, if it exists in Nature, means that we can reject both the CP-conserving values of 0° , 180° at a given confidence level. Obviously, this measurement becomes very difficult when δ_{CP} approaches to 0° , 180° . Therefore, whilst it is possible to discover the mass hierarchy for *all* possible values of δ_{CP} , the same is not true in the case of CP violation study. We have already emphasized that the present uncertainty in the knowledge of $\sin^2\theta_{23}$ has a crucial impact on the discovery reach of mass ordering and octant of θ_{23} for the experimental setups under consideration. This is also true for the CP violation discovery reach. We can see from the appearance probability expression in

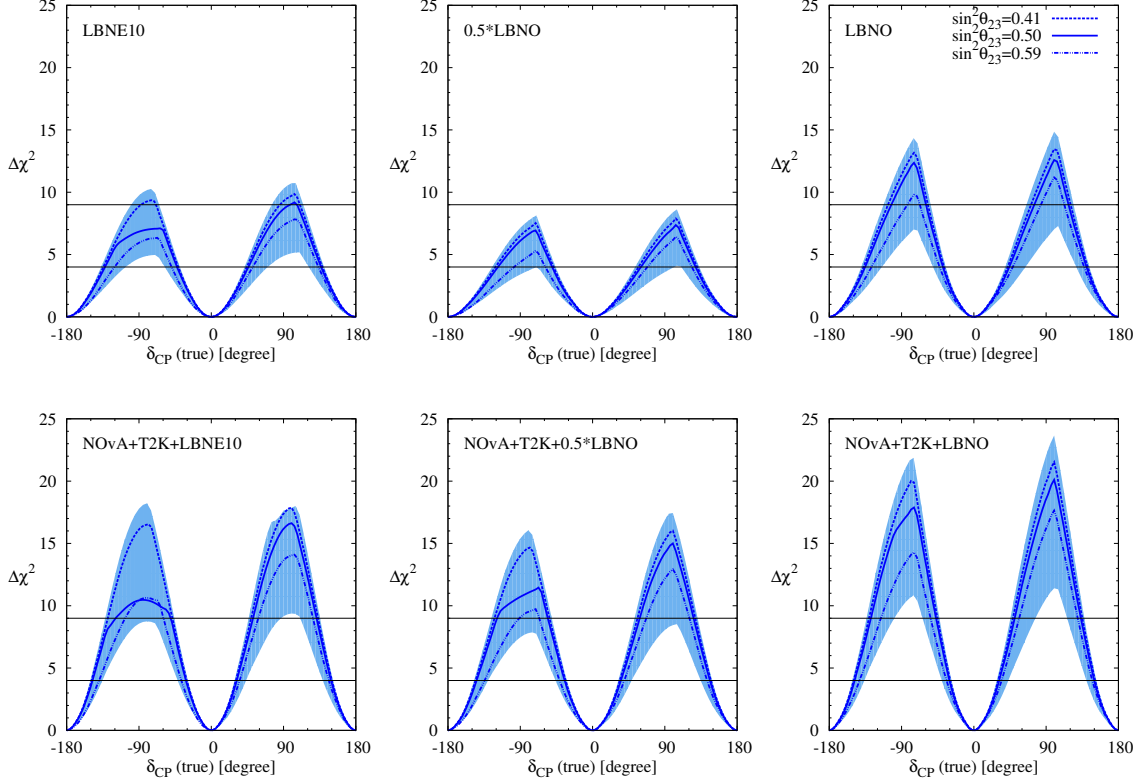


Figure 8: CP Violation discovery reach as a function of true value of δ_{CP} assuming NH as true hierarchy. Results are shown for LBNE10 (10 kt), 0.5*LBNO (10 kt), and LBNO (20 kt) setups in the left, middle, and right upper panels respectively. In lower panels, we show the same including the projected data from T2K and NO ν A experiments. The shaded band depicts the variation in $\Delta\chi^2_{\text{min}}$ due to different true choices of $\sin^2\theta_{23}$ in its 3σ allowed range of 0.34 to 0.67. Inside the band, we show the results for three different true values of $\sin^2\theta_{23}$: 0.41, 0.5, and 0.59.

equation 2.2 that both the CP-violating (C_-) and CP-conserving (C_+) terms depend on $\sin 2\theta_{23}$, therefore these terms are not sensitive to the octant of θ_{23} but they depend on the value of θ_{23} . The leading term (C_0) in equation 2.2 is proportional to $\sin^2\theta_{23}$ and therefore it is sensitive to both the octant and magnitude of θ_{23} . In this paper for the first time, we study in detail the CP violation discovery reach by varying the true value of $\sin^2\theta_{23}$ in its allowed 3σ range of 0.34 to 0.67. We follow the same marginalization scheme in the fit for oscillation parameters and systematic uncertainties as that in the case of mass hierarchy discovery study. For CP violation searches, the final $\Delta\chi^2$ is also marginalized over both the choices of hierarchy in the fit to obtain $\Delta\chi^2_{\text{min}}$.

In figure 8, we present the CP violation discovery reach for various experimental setups under consideration as a function of true δ_{CP} assuming NH as true hierarchy. Similar figure for the true IH choice is given in appendix B. The left, middle, and right upper panels of figure 8 show the results for LBNE10, 0.5*LBNO, and LBNO respectively. In lower panels, we depict the same results, combining the projected data from T2K and NO ν A experiments. The shaded band in each panel reflects the variation in $\Delta\chi^2_{\text{min}}$ due to different true choices of $\sin^2\theta_{23}$ in its 3σ allowed range of 0.34 to 0.67. Inside the band, we give

Setups	Fraction of $\delta_{\text{CP}}(\text{true})$	
	2σ confidence level	3σ confidence level
LBNE10 (10 kt)	0.51	0.03
LBNE10 + T2K + NO ν A	0.63	0.43
0.5*LBNO (10 kt)	0.40	0.0
0.5*LBNO + T2K + NO ν A	0.63	0.37
LBNO (20 kt)	0.51	0.23
LBNO + T2K + NO ν A	0.69	0.46

Table 1: Fraction of $\delta_{\text{CP}}(\text{true})$ for which a discovery is possible for CP violation considering NH as true hierarchy. Here, we assume maximal mixing for the true choice of θ_{23} . The results are presented at 2σ and 3σ confidence level.

the results for three different true values of $\sin^2 \theta_{23}$: 0.41, 0.5, and 0.59. We summarize the main features of figure 8 in Table 1. In their first phases, both LBNE10 and LBNO will have CP violation reach for around 50% values of true δ_{CP} at 2σ confidence level (see Table 1). At 3σ , their CP violation reach is quite minimal: only 3% for LBNE10 and 23% for LBNO. It is quite important to note that the addition of the projected T2K and NO ν A data helps a lot to improve the CP coverage for these setups at 3σ confidence level for all possible true values of $\sin^2 \theta_{23}$ (see figure 8). For an example, LBNE10 (LBNO) can achieve CP violation discovery for 43% (46%) values of true δ_{CP} at 3σ combining the expected data from the current generation experiments T2K and NO ν A assuming $\sin^2 \theta_{23}(\text{true}) = 0.5$. For 0.5*LBNO, we do not have any sensitivity at 3σ C.L. but, adding the T2K and NO ν A data, 37% CP coverage can be obtained. All these results again clearly demonstrate that the projected data from the current generation off-axis superbeam experiments will be quite useful for future generation on-axis wide band superbeam setups to enhance their discovery reach at higher confidence level. Another important feature that emerges from figure 8 is that the CP violation discovery reach is quite sensitive to the true value of $\sin^2 \theta_{23}$. The results are better if $\sin^2 \theta_{23}(\text{true})$ belongs to LO compared to HO. The main reason behind this is that like in the case of θ_{13} [66, 67], the CP-asymmetry increases if we lower the value of θ_{23} , reducing the strength of the leading term (C_0) in equation 2.2.

6 Concluding Remarks

With the recent measurement of θ_{13} by reactor experiments, a clear and comprehensive picture of the three flavor leptonic mixing matrix has been established. This impressive result has crucial consequences for future theoretical and experimental efforts. It has opened up the possibility to probe the sub-dominant three flavor effects in both current and future long-baseline oscillation facilities. Another interesting piece of information on θ_{23} has been provided by recently completed MINOS accelerator experiment. $\nu_\mu \rightarrow \nu_\mu$ disappearance data of MINOS points towards the deviation from maximal 2-3 mixing, causing the octant

ambiguity of θ_{23} . In this paper, we present a comparative study of the physics reach of two future superbeam facilities, LBNE and LBNO in their first phases of run, in addressing the issues of neutrino mass hierarchy, octant of θ_{23} , and leptonic CP violation. We also demonstrate that the projected data from current generation experiments, T2K and NO ν A will play a crucial role for these future facilities to achieve their milestones with higher confidence level. Also for the first time, we study in detail the impact of the present uncertainty in 2-3 mixing angle in resolving these fundamental issues.

We find that in its first phase, even a 50% scaled down version of LBNO with 10 kt detector mass has more than 7σ mass hierarchy discovery reach for the lowest possible value of $\sin^2 \theta_{23}(\text{true}) = 0.34$ in its presently allowed 3σ range. This result is valid for any choices of true δ_{CP} and hierarchy. However, LBNE10 suffers in this regard and will not be able to provide a 5σ result for about 50% of the true δ_{CP} range even for maximal mixing choice for $\sin^2 \theta_{23}(\text{true})$. Moreover, it fails to achieve even a 3σ hierarchy discovery for the best-fit value in LO, $\sin^2 \theta_{23}(\text{true}) = 0.41$ and the worst case combinations of the true parameters (NH, 90°) and (IH, -90°). In such a scenario, the projected data from T2K and NO ν A can be extremely useful for LBNE10. Adding the expected informations from T2K and NO ν A, LBNE10 can discover mass hierarchy at 3σ confidence level for any combinations of true hierarchy- δ_{CP} and even for the most conservative choice of $\sin^2 \theta_{23}(\text{true}) = 0.34$ in its present 3σ range. It clearly corroborates the synergy between the current (off-axis) and future (on-axis) superbeam experiments.

As far as the octant discovery is concerned, adding the projected data from equal neutrino and anti-neutrino runs of T2K (2.5 years each) and NO ν A (3 years each), LBNE10 can provide a 3σ octant resolution for $\sin^2 \theta_{23}(\text{true}) \leq 0.44$ and for $\sin^2 \theta_{23}(\text{true}) \geq 0.58$ for all values of $\delta_{\text{CP}}(\text{true})$. For 0.5*LBNO, this is possible for $\sin^2 \theta_{23}(\text{true}) \leq 0.45$ and for $\sin^2 \theta_{23}(\text{true}) \geq 0.57$.

In their first phases, both LBNE10 and LBNO can establish leptonic CP violation for around 50% values of true δ_{CP} at 2σ confidence level. At 3σ , their CP violation reach is quite minimal: only 3% for LBNE10 and 23% for LBNO. The expected measurements from present generation experiments T2K and NO ν A can have dramatic impact on the CP violation discovery reach of the future facilities in their first phases of run. In case of LBNE10, CP coverage can be enhanced from 3% to 43% at 3σ combining T2K and NO ν A data assuming $\sin^2 \theta_{23}(\text{true}) = 0.5$. For LBNO setup, CP violation discovery is possible for 46% values of true δ_{CP} at 3σ if we add the data from T2K and NO ν A.

Acknowledgments

We would like to thank M. Bishai, G. Zeller, A. Rubbia and M. Goodman for helpful communications. SKA was supported by the DST/INSPIRE Research Grant [IFA-PH-12], Department of Science and Technology, India.

A Resolution of Octant as a function of true θ_{23} for IH(true)

In this appendix, we present the results for octant discovery generating the data with IH. In figure 9, we show the $\Delta\chi_{\text{min}}^2$ as a function of true $\sin^2 \theta_{23}$ for LBNE10 (left panel) and

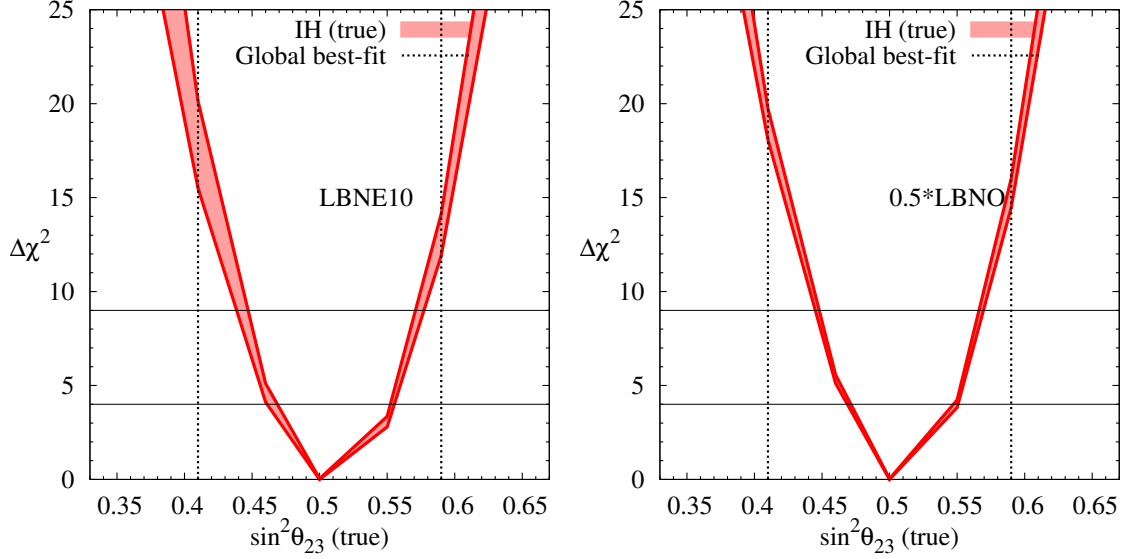


Figure 9: $\Delta\chi^2_{\min}$ for octant resolution as a function of true $\sin^2\theta_{23}$. Left panel (right panel) is for LBNE10 (0.5*LBNO). The variation due to $\delta_{\text{CP}}(\text{true})$ leads to the band in $\Delta\chi^2$ for a given $\sin^2\theta_{23}(\text{true})$. The vertical lines correspond to the global best-fit values. We consider IH as true hierarchy. In producing all these plots, the projected data from T2K and NO ν A have been added (see section 3 for details).

0.5*LBNO (right panel) assuming IH as true hierarchy. Variation of $\delta_{\text{CP}}(\text{true})$ in the range -180° to 180° leads to the band in $\Delta\chi^2$ values for a given true $\sin^2\theta_{23}$. The vertical lines indicate towards the global best-fit values. Here we add the projected data from T2K and NO ν A to produce these results. For LBNE10, a 3σ octant resolution is possible for $\sin^2\theta_{23}(\text{true}) \leq 0.44$ and for $\sin^2\theta_{23}(\text{true}) \geq 0.58$ irrespective of the values of $\delta_{\text{CP}}(\text{true})$. For 0.5*LBNO, this is possible for $\sin^2\theta_{23}(\text{true}) \leq 0.44$ and for $\sin^2\theta_{23}(\text{true}) \geq 0.57$. We see that the results with IH(true) choice are quite similar to that of NH(true) (see figure 6).

Figure 10 shows the 3σ and 5σ octant resolution contours in true $\sin^2\theta_{23}$ - true δ_{CP} plane considering IH as true hierarchy. The left (right) panel is for LBNE10 (0.5*LBNO) adding the expected data from T2K and NO ν A. Octant resolution is only possible for points lying outside the contours. This figure again suggests that for IH(true) case, both LBNE10 and 0.5*LBNO in combination with T2K and NO ν A data can provide octant discovery for global best-fit points at 3σ confidence level.

B CP Violation discovery as a function of true δ_{CP} for IH(true)

In figure 11, we give the CP violation discovery reach for various experimental setups under study as a function of true δ_{CP} considering IH as true hierarchy. Like in figure 8, the left, middle, and right upper panels of figure 11 present the results for LBNE10, 0.5*LBNO, and LBNO respectively. In lower panels, we depict the same combining the projected data from T2K and NO ν A experiments. The shaded band in each panel reflects the variation in $\Delta\chi^2_{\min}$ due to different true choices of $\sin^2\theta_{23}$ in its 3σ allowed range of 0.34 to 0.67. Inside the band, we give the results for three different true values of $\sin^2\theta_{23}$: 0.41, 0.5, and

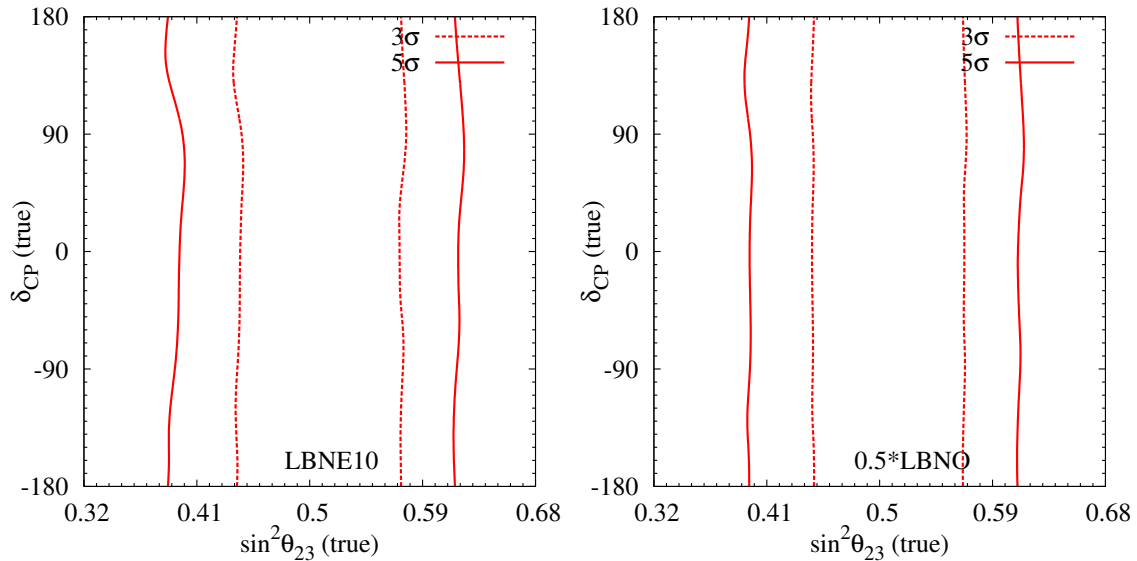


Figure 10: Octant resolving capability at 3σ and 5σ C.L. in the true $\sin^2\theta_{23}$ - true δ_{CP} plane for LBNE10 (left panel) and $0.5*LBNO$ (right panel). The vertical lines point towards the global best-fit values. Here, we assume IH as true hierarchy. In generating all these plots, the projected data from T2K and NO ν A have been added (see section 3 for details).

0.59. We do not see any qualitative differences in the CP violation discovery reach for these setups when we generate the data assuming IH instead of NH. Around $\delta_{CP}(\text{true}) = \pm 90^\circ$ (where CP violation is maximum), the results are slightly better for NH(true) compared to IH(true).

References

- [1] F. An *et al.* (Daya Bay Collaboration) (2013), [1310.6732](#).
- [2] F. An *et al.* (Daya Bay Collaboration), Phys.Rev.Lett. **108**, 171803 (2012), [1203.1669](#).
- [3] J. Ahn *et al.* (RENO), Phys.Rev.Lett. **108**, 191802 (2012), [1204.0626](#).
- [4] Y. Abe *et al.* (Double Chooz), Phys.Rev. **D86**, 052008 (2012), [1207.6632](#).
- [5] R. Nichol (MINOS Collaboration), Nucl.Phys.Proc.Suppl. **235-236**, 105 (2013).
- [6] P. Adamson *et al.* (MINOS Collaboration), Phys. Rev. Lett. **110**, **251801** (2013), [1304.6335](#).
- [7] A. Osipowicz *et al.* (KATRIN Collaboration) (2001), [hep-ex/0109033](#).
- [8] I. Avignone, Frank T., S. R. Elliott, and J. Engel, Rev.Mod.Phys. **80**, 481 (2008), [0708.1033](#).
- [9] J. Lesgourgues and S. Pastor, Adv.High Energy Phys. **2012**, 608515 (2012), [1212.6154](#).
- [10] P. Ade *et al.* (Planck Collaboration) (2013), [1303.5076](#).
- [11] D. Forero, M. Tortola, and J. Valle, Phys.Rev. **D86**, 073012 (2012), [1205.4018](#).
- [12] G. Fogli, E. Lisi, A. Marrone, D. Montanino, A. Palazzo, *et al.*, Phys.Rev. **D86**, 013012 (2012), [1205.5254](#).

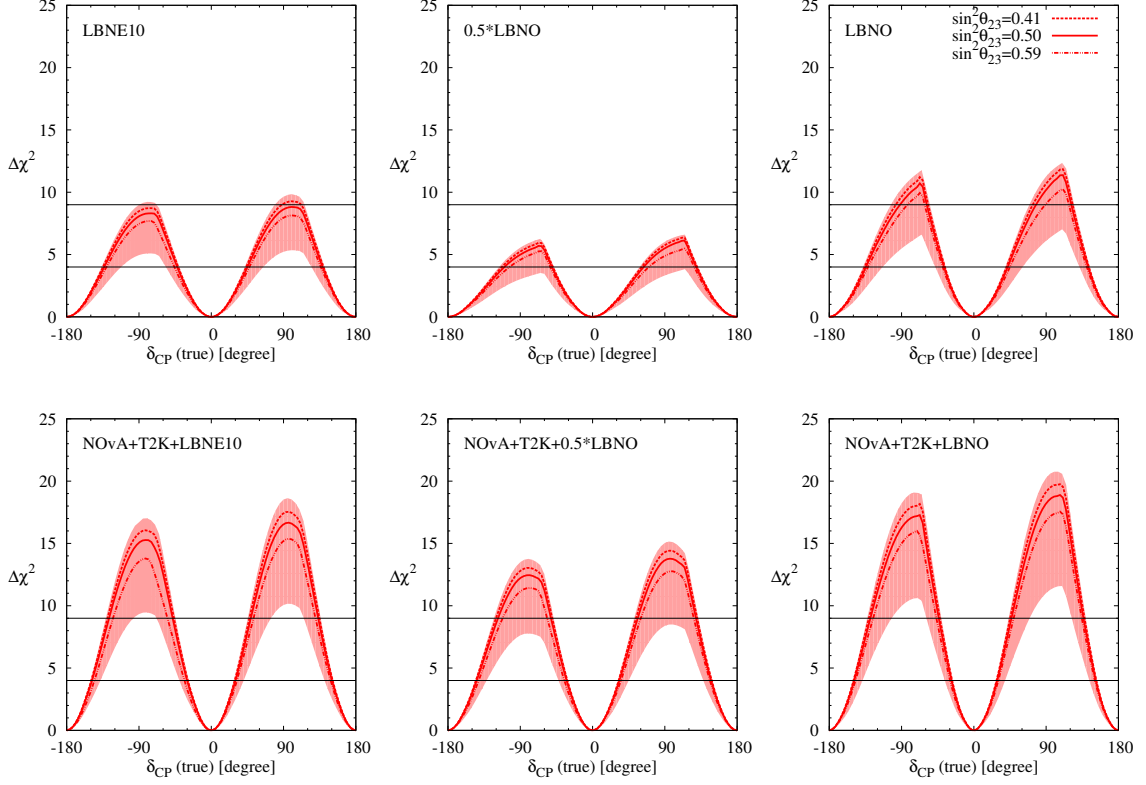


Figure 11: CP Violation discovery reach as a function of true value of δ_{CP} assuming IH as true hierarchy. Results are shown for LBNE10 (10 kt), 0.5*LBNO (10 kt), and LBNO (20 kt) in the left, middle, and right upper panels respectively. In lower panels, we depict the same adding the information from T2K and NO ν A experiments. The shaded band depicts the variation in $\Delta\chi^2_{\text{min}}$ due to different true choices of $\sin^2\theta_{23}$ in its 3σ allowed range of 0.34 to 0.67. Inside the band, we show the results for three different true values of $\sin^2\theta_{23}$: 0.41, 0.5, and 0.59.

- [13] M. Gonzalez-Garcia, M. Maltoni, J. Salvado, and T. Schwetz, JHEP **1212**, 123 (2012), [1209.3023](#).
- [14] C. H. Albright and M.-C. Chen, Phys.Rev. **D74**, 113006 (2006), [hep-ph/0608137](#).
- [15] S. Pascoli, S. Petcov, and T. Schwetz, Nucl.Phys. **B734**, 24 (2006), [hep-ph/0505226](#).
- [16] M. Fukugita and T. Yanagida, Phys.Lett. **B174**, 45 (1986).
- [17] R. N. Mohapatra and S. Nussinov, Phys.Rev. **D60**, 013002 (1999), [hep-ph/9809415](#).
- [18] K. Babu, E. Ma, and J. Valle, Phys.Lett. **B552**, 207 (2003), [hep-ph/0206292](#).
- [19] H. Minakata and A. Y. Smirnov, Phys.Rev. **D70**, 073009 (2004), [hep-ph/0405088](#).
- [20] L. J. Hall, H. Murayama, and N. Weiner, Phys.Rev.Lett. **84**, 2572 (2000), [hep-ph/9911341](#).
- [21] A. de Gouvea and H. Murayama (2012), [1204.1249](#).
- [22] Y. Itow *et al.* (T2K Collaboration) pp. 239–248 (2001), [hep-ex/0106019](#).
- [23] K. Abe *et al.* (T2K Collaboration), Nucl.Instrum.Meth. **A659**, 106 (2011), [1106.1238](#).
- [24] D. Ayres, G. Drake, M. Goodman, V. Guarino, T. Joffe-Minor, *et al.* (2002), [hep-ex/0210005](#).

- [25] D. Ayres *et al.* (NOvA Collaboration) (2004), updated version of 2004 proposal. Higher resolution version available at Fermilab Library Server, [hep-ex/0503053](#).
- [26] D. Ayres *et al.* (NOvA Collaboration) (2007).
- [27] S. K. Agarwalla, S. Prakash, S. K. Raut, and S. U. Sankar, JHEP **1212**, 075 (2012), [1208.3644](#).
- [28] S. K. Agarwalla, S. Prakash, and S. U. Sankar, JHEP **1307**, 131 (2013), [1301.2574](#).
- [29] A. Chatterjee, P. Ghoshal, S. Goswami, and S. K. Raut, JHEP **1306**, 010 (2013), [1302.1370](#).
- [30] M. Diwan, D. Beavis, M.-C. Chen, J. Gallardo, S. Kahn, *et al.*, Phys.Rev. **D68**, 012002 (2003), [hep-ph/0303081](#).
- [31] V. Barger, M. Bishai, D. Bogert, C. Bromberg, A. Curioni, *et al.* (2007), [0705.4396](#).
- [32] P. Huber and J. Kopp, JHEP **1103**, 013 (2011), [1010.3706](#).
- [33] T. Akiri *et al.* (LBNE Collaboration) (2011), corresponding author R.J.Wilson (Bob.Wilson@colostate.edu)/ 113 pages, 90 figures, [1110.6249](#).
- [34] C. Adams *et al.* (LBNE Collaboration) (2013), [1307.7335](#).
- [35] D. Autiero, J. Aysto, A. Badertscher, L. B. Bezrukov, J. Bouchez, *et al.*, JCAP **0711**, 011 (2007), [0705.0116](#).
- [36] A. Rubbia (2010), [1003.1921](#).
- [37] D. Angus *et al.* (LAGUNA Collaboration) (2010), [1001.0077](#).
- [38] A. Rubbia (LAGUNA Collaboration), Acta Phys.Polon. **B41**, 1727 (2010).
- [39] A. Stahl, C. Wiebusch, A. Guler, M. Kamiscioglu, R. Sever, *et al.* (2012).
- [40] L. Wolfenstein, Phys.Rev. **D17**, 2369 (1978).
- [41] S. P. Mikheev and A. Y. Smirnov, Sov. J. Nucl. Phys. **42**, 913 (1985), [Yad.Fiz.42:1441-1448,1985].
- [42] V. D. Barger, K. Whisnant, S. Pakvasa, and R. J. N. Phillips, Phys. Rev. **D22**, 2718 (1980).
- [43] A. Cervera *et al.*, Nucl. Phys. **B579**, 17 (2000), [Erratum-ibid.B593:731-732,2001], [hep-ph/0002108](#).
- [44] M. Freund, P. Huber, and M. Lindner, Nucl. Phys. **B615**, 331 (2001), [hep-ph/0105071](#).
- [45] E. K. Akhmedov, R. Johansson, M. Lindner, T. Ohlsson, and T. Schwetz, JHEP **0404**, 078 (2004), [hep-ph/0402175](#).
- [46] H. Minakata and H. Nunokawa, JHEP **10**, 001 (2001), [hep-ph/0108085](#).
- [47] A. Para and M. Szeleper (2001), [hep-ex/0110032](#).
- [48] M. Fechner Presented on 9 May 2006.
- [49] P. Huber, M. Lindner, T. Schwetz, and W. Winter, JHEP **0911**, 044 (2009), [0907.1896](#).
- [50] R. Patterson (NOvA Collaboration), Nucl.Phys.Proc.Suppl. **235-236**, 151 (2013), [1209.0716](#).
- [51] Mary Bishai, private communication (2012).
- [52] S. K. Agarwalla, T. Li, and A. Rubbia, JHEP **1205**, 154 (2012), [1109.6526](#).
- [53] Geralyn Zeller, private communication (2012).

- [54] R. Petti and G. Zeller, *Nuclear Effects in Water vs. Argon*, Tech. Rep. LBNE docdb No. 740.
- [55] Silvestro di Luise (2012), Poster presented at the ICHEP2012 Conference, July 4-11, 2012, Melbourne, Australia, www.ichep2012.com.au/.
- [56] P. Huber, M. Lindner, and W. Winter, *Comput.Phys.Commun.* **167**, 195 (2005), [hep-ph/0407333](https://arxiv.org/abs/hep-ph/0407333).
- [57] P. Huber, J. Kopp, M. Lindner, M. Rolinec, and W. Winter, *Comput.Phys.Commun.* **177**, 432 (2007), [hep-ph/0701187](https://arxiv.org/abs/hep-ph/0701187).
- [58] H. Nunokawa, S. J. Parke, and R. Zukanovich Funchal, *Phys.Rev.* **D72**, 013009 (2005), [hep-ph/0503283](https://arxiv.org/abs/hep-ph/0503283).
- [59] A. de Gouvea, J. Jenkins, and B. Kayser, *Phys.Rev.* **D71**, 113009 (2005), [hep-ph/0503079](https://arxiv.org/abs/hep-ph/0503079).
- [60] M. Blennow, P. Coloma, A. Donini, and E. Fernandez-Martinez, *JHEP* **1307**, 159 (2013), [1303.0003](https://arxiv.org/abs/1303.0003).
- [61] X. Qian (Daya Bay) (2012), talk given at the NuFact 2012 Conference, July 23-28, 2012, Williamsburg, USA, <http://www.jlab.org/conferences/nufact12/>.
- [62] X. Qian, A. Tan, W. Wang, J. Ling, R. McKeown, *et al.*, *Phys.Rev.* **D86**, 113011 (2012), [1210.3651](https://arxiv.org/abs/1210.3651).
- [63] S. K. Raut, R. S. Singh, and S. U. Sankar, *Phys.Lett.* **B696**, 227 (2011), [0908.3741](https://arxiv.org/abs/0908.3741).
- [64] A. Dighe, S. Goswami, and S. Ray, *Phys.Rev.Lett.* **105**, 261802 (2010), [1009.1093](https://arxiv.org/abs/1009.1093).
- [65] S. Prakash, S. K. Raut, and S. U. Sankar, *Phys.Rev.* **D86**, 033012 (2012), [1201.6485](https://arxiv.org/abs/1201.6485).
- [66] K. Dick, M. Freund, M. Lindner, and A. Romanino, *Nucl.Phys.* **B562**, 29 (1999), [hep-ph/9903308](https://arxiv.org/abs/hep-ph/9903308).
- [67] A. Donini, M. Gavela, P. Hernandez, and S. Rigolin, *Nucl.Phys.* **B574**, 23 (2000), [hep-ph/9909254](https://arxiv.org/abs/hep-ph/9909254).